Supplementary information

A Chemical Toolbox for the Study of Bromodomains and Epigenetic Signaling

Knapp and Arrowsmith et al.

Content:

Supplementary figure 1

CBP30-298

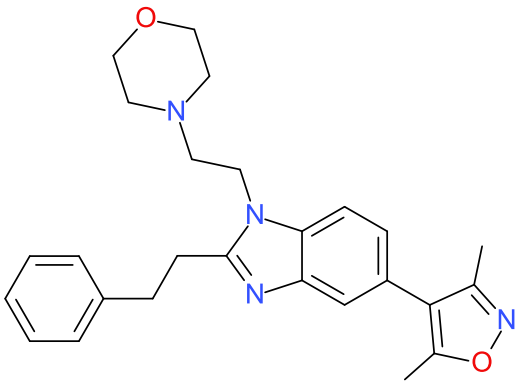

CBP30-383

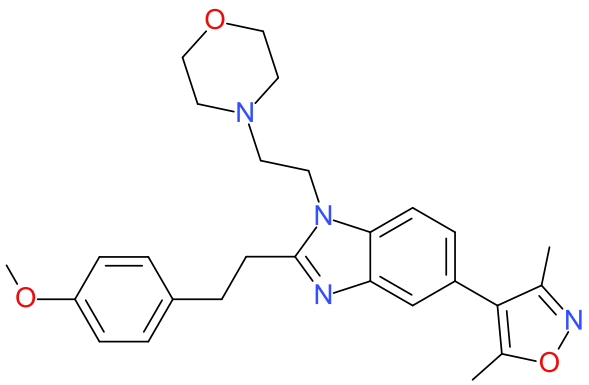

PFI-3 D1

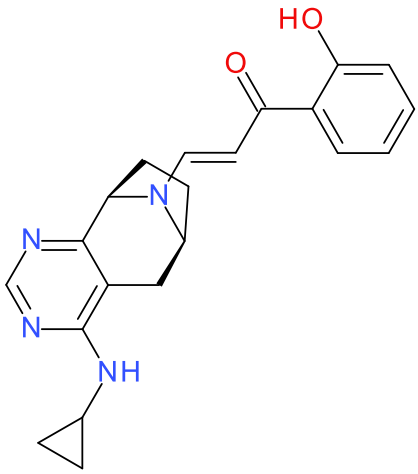

BAY-876

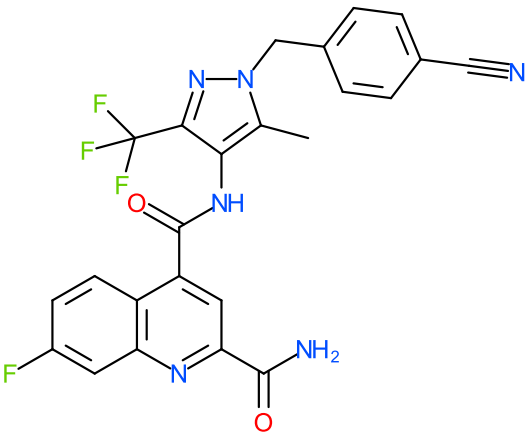

Supplementary figure 1: Chemical Structures of probe related compounds and BAY-876.

Supplementary Figure 2

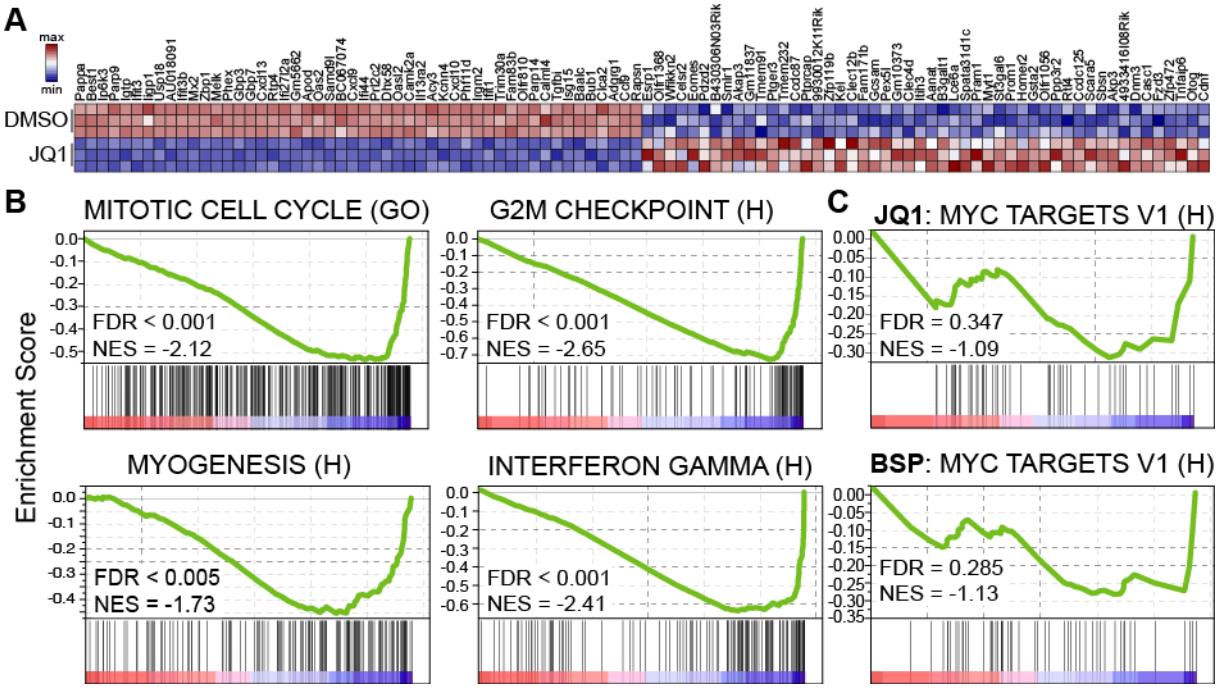

Supplementary Figure 2: Transcriptional response to BSP and JQ1 in C2C12 myoblasts. **A)** Heatmap of the top 50 up/down regulated genes in C2C12 myoblasts following 12 h JQ1 treatment based on 2-sided signal to noise ratio (SNR) score and $P < 0.05$. Dark blue indicates lowest expression; dark red indicates highest expression, with intermediate values represented by lighter shades, as indicated in the inset. Data are column-normalized. **B)** GSEA demonstrating strong association with mitotic cell cycle (from the Gene Ontology MSigDB set, top left), G2M checkpoint (from hallmark MSigDB signatures, top-right), myogenesis (from hallmark MSigDB signatures, bottom-left) and interferon gamma signalling, following 12 h treatment of C2C12 cells with JQ1. **C)** GSEA demonstrating lack of association with MYC response following 12 h treatment of C2C12 cells with JQ1 (top panel) and BSP (lower panel).

Supplementary Figure 3

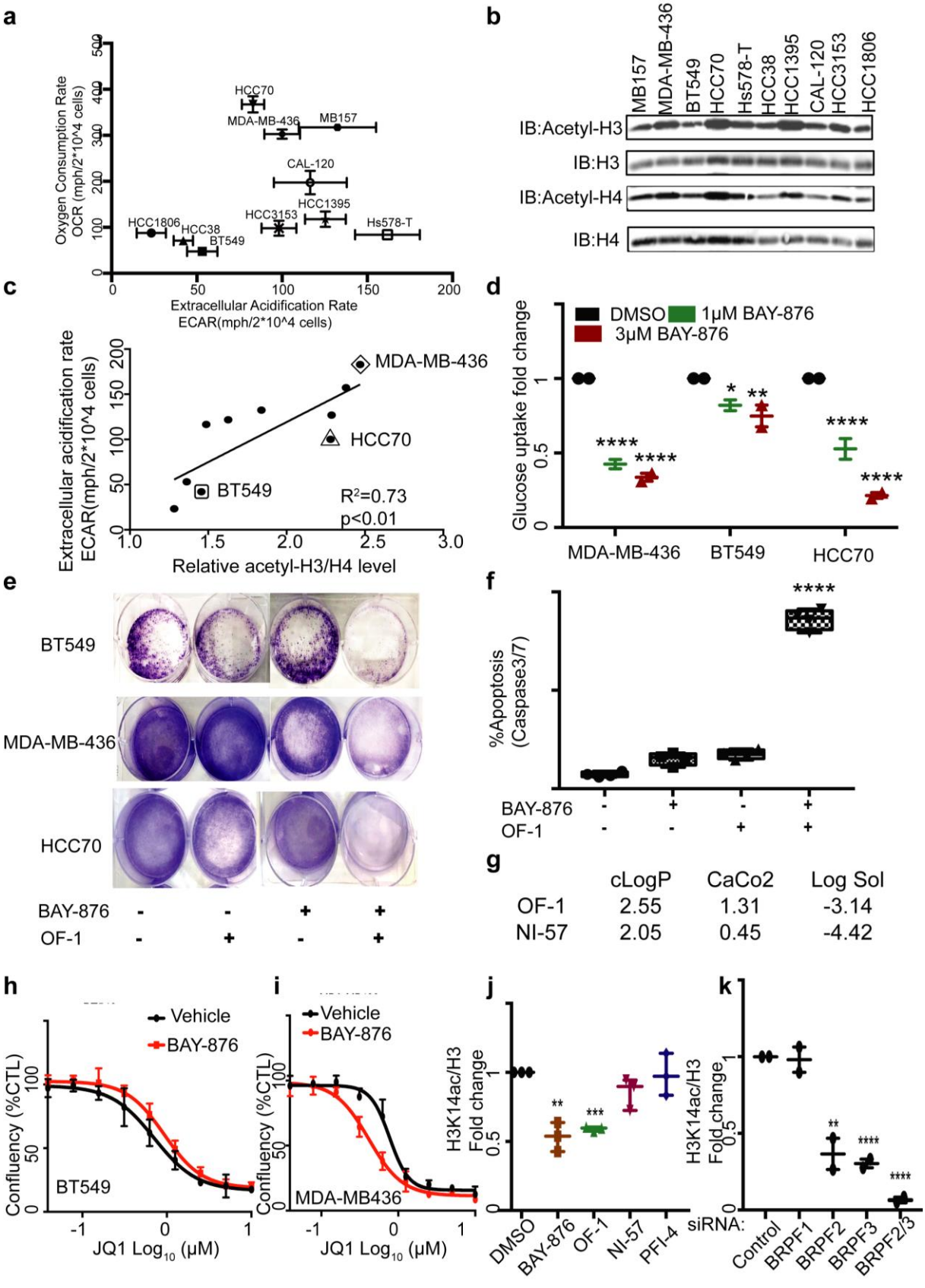

Supplementary Figure 3: Metabolic profiles and synergy with of BRPF bromodomain inhibition with BAY-876 a) Metabolic profiles of ten TNBC lines based on Seahorse XF96 measurements. Depicted are the ECAR (X axis) and the OCR (Y axis) measurements. Graph

indicate mean and error bars denote standard deviation from eight wells (from two independent assays). **b)** A representative immunoblot of histone acetylation level across ten TNBC lines. **c)** Plot of ECAR and histone acetylation across ten TNBC lines. Labeled dots denote the representative TNBC lines, having extreme or medial glycolytic rates and histone acetylation levels, used for the following assays. **d)** Glucose uptake in three representative cell lines in respond to BAY-876 treatment relative to vehicle. Experiment repeated two times. Cells were treated with DMSO or indicated concentration of BAY-876 for 5 days. Graph indicate mean and error bars denote standard deviation from three independent assays. p value computed using a one-way ANOVA test; ****** p<0.001. **e)** The colony formation of indicated cells with 3μM indicated chemical probes treatment for 14 days. **f)** MDA-MB436 cells were treated with 3μM indicated chemical probes for 5 days. Cell apoptotic activity was quantified by the fluorescent caspase 3/7 active objects. Graph indicate mean and error bars denote standard deviation from four independent assays. p value computed using one-way ANOVA t test; **** p<0.001. **g)** Pharmacokinetic properties of NI-57 and OF-1 predicted by pkCSM (http://biosig.unimelb.edu.au/pkcsm/prediction). **h)** Dose dependent curves for cell lines treated with indicated concentrations of JQ-1 with or without 3μM BAY876 for 7 days in BT549 cell line. Graph indicate mean and error bars denote standard deviation from four independent assays. p value computed using a two- stage step-up Benjamini t test **i)** Dose dependent curves for cell lines treated with indicated concentrations of JQ-1 with or without 3μM BAY876 for 7 days in MDA-MB-436 cell line. Graph indicate mean and error bars denote standard deviation from four independent assays. p value computed using a two- stage step-up Benjamini t test **j)** Immunoblot based quantification of H3K14ac abundance using total H3 as a control in MDA-MB-436 cells following control or 3 μM of the indicated chemical probes during a 5-day treatment. Graph indicate mean and error bars denote standard deviation from three independent assays. p value computed using a two-stage step-up Benjamini t test; **p<0.01; *** p<0.001. **k)** Immunoblot based quantification of H3K14ac abundance using total H3 as a control in MDA-MB-436 BRPF knockdown cells. Graph indicate mean and error bars denote standard deviation from two independent assays. p value computed using a two-stage step-up Benjamini t test; **p<0.01; *** p<0.001.

Supplementary Table 1: Probe set for the human bromodomain family

Target	Inhibitor Negative control Supplier‡	SMILE	K_D (nM)	Ref.
Family I: PCAF/GCN5	**L-Moses** **Negative control: D-Moses** **Probe: T** **Control: SGC**	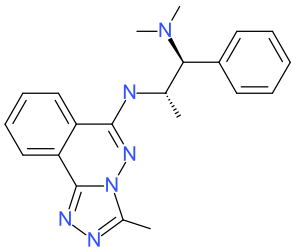	ITC data: 126 nM PCAF 600 nM GCN5	**1**
Family I: PCAF/GCN5	**GSK4027** **Negative control: GSK4028** **SGC**	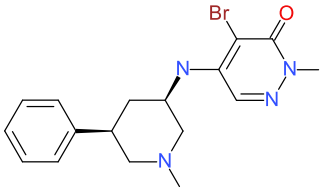	BROMOscan 1.4nM PCAF 1.4nM GCN5	**2**
Family I: CECR2	**NVS-CECR2-1** **C, M, T**	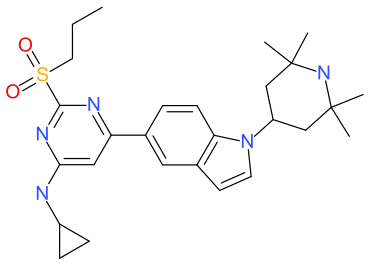	ITC data: 80nM CECR2	**3**
Family I: CECR2	**GNE-886** **MedKoo**	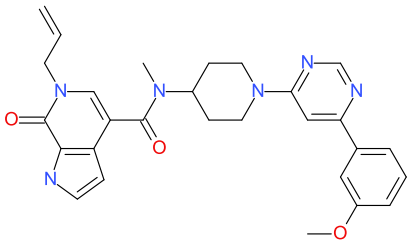	EC_{50} 370nM CECR2	**4**
Family 2 BET (BRD4, 3, 2,T)	**(+)-JQ1** **Negative control: (-)-JQ1** **C, M, T**	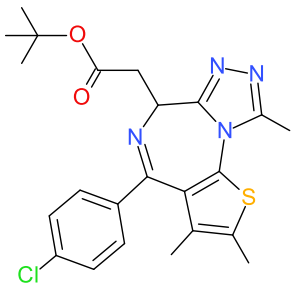	ITC data: 49nM BRD4(1) 90nM BRD4(2) 59nM BRD3(1) 82nM BRD3(2) 128nM BRD2(1) 190nM BRDT(1)	**5**
Family 2 BET (BRD4, 3, 2,T)	**I-BET151** **C, T**	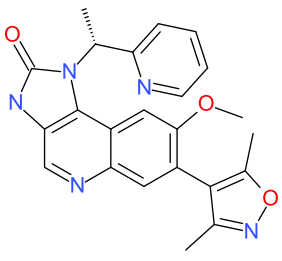	Cell free assay IC50 of 500 nM, 25 nM, and 790nM	**6**

Family 2 BET (BRD4, 3, 2,T)	**PFI-1** **C, M, T**	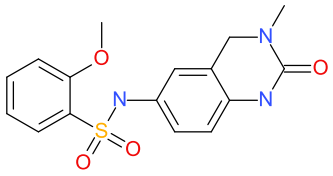	ITC data: 47nM BRD4(1) 195nM BRD4(2) 80nM BRD3(1) 76nM BRD3(2) 108nM BRD2(1) 144nM BRD2(2) 85nM BRDT(1) 221nM BRDT(2)	**7**
Family III CBP/p300	**SGC-CBP30** **Negative control: BDOIA513** **Probe: C, M, T** **Control: SGC**	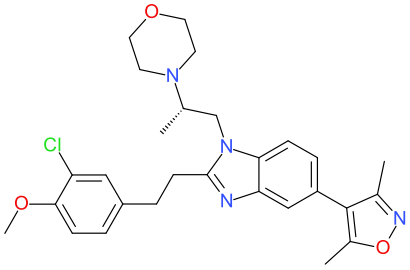	ITC data: 21nM CBP 38nM p300	**8**
Family III CBP/p300	**I-CBP112** **C, M, T**	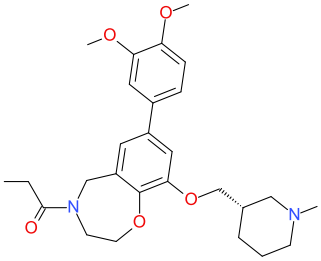	ITC data: 151nM CBP 625nM p300	**9**
Family III CBP/p300	**GNE-781** **MedKoo**	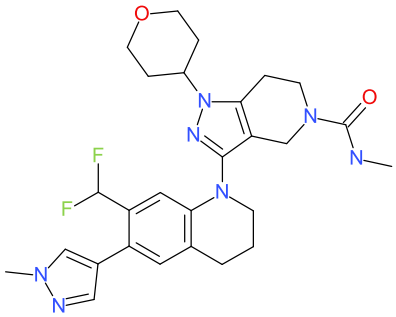	TR-FRET: 0.94 nM BRET: 6.2 nM	**10**
Family IV pan-BRPF	**OF-1** **C, M, T**	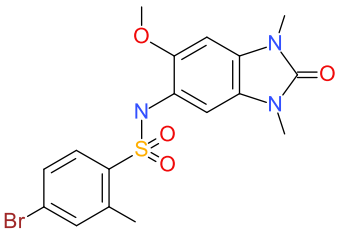	ITC data: 101nM BRPF1B 505nM BRPF2 2400nM BRPF3 Off target BRD4(1) 3900 nM	**11**

Family IV pan-BRPF	**GSK6853** **Negative control: GSK9311** **Probe: C, M** **Control: M**	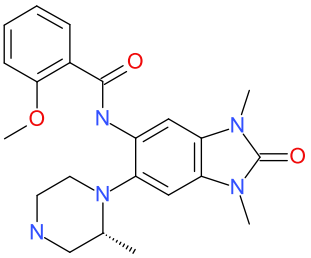	TR-FRET 81nM BRPF1B	**12**
Family IV pan-BRPF	**NI-57** **C, M, T**	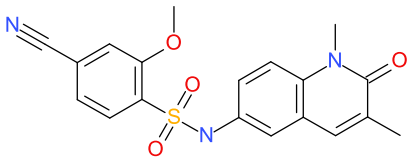	ITC data: 31nM BRPF1B 108nM BRPF2 409nM BRPF3 Off target BRD9 998nM	**11**
Family IV BRPF1B	**PFI-4** **C, M, T**	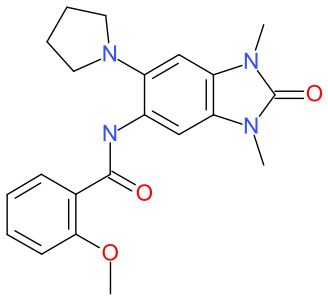	ITC data: 13nM BRPF1B 775nM BRPF2 Off target CECR2 2350nM	**11**
Family IV BRPF2 **Family VII TAF1(2) TAf1L(2)**	**BAY-299** **Negative control: BAY-364** **C, M, T**	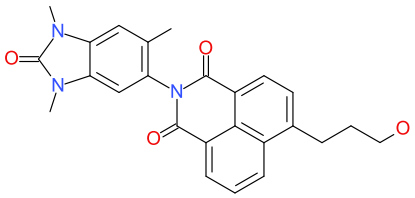	ITC data: 44nM BRPF2 16nM TAF1(2) 234nM TAF1L(2) Off target 1390nM CBP	**13**
Family IV BRD7/BRD9	**TP-472** **Negative control: TP-472N** **C, M, T**	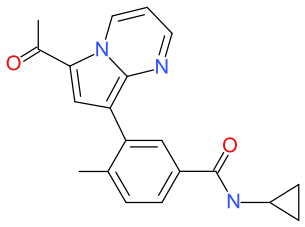	ITC data: 33nM BRD9 340nM BRD7	**14**
Family IV BRD7/BRD9	**BI-9564** **C, M, T**	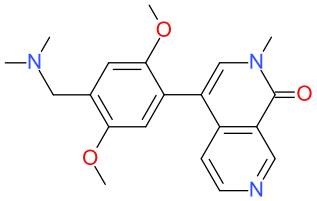	ITC data: 15nM BRD9 BROMOscan 0.75nM BRD9 0.3 nM BRD7 Off target ITC CECR2: 187nM	**15**

Family IV BRD7/BRD9	**LP-99** **Negative control: (2S,3R)-LP99** **Probe: C, M, T** **Control: SGC**	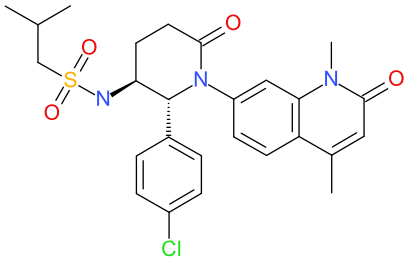	ITC data: 99nM BRD9 909nM BRD7	**16**
Family IV BRD7/BRD9	**I-BRD9** **C, M, T**	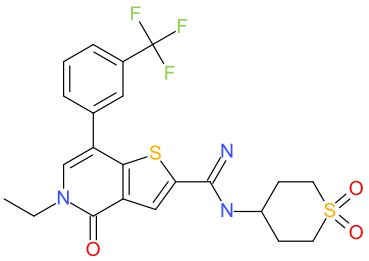	BROMOscan: 1.9 nM BRD9 380nM BRD7 Off target CECR2 140nM CBP 740nM p300 770nM BRPF1 2100nM	**17**
(BRPF1B) (ATAD2 8Family IV ATAD2B	**GSK8814** **Negative control: GSK8815** **SGC**	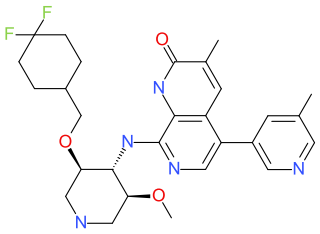	ITC 10 nM ATAD2B	**18**
Family IV and VI TRIM24 BRPF1	**Benzimidazolone 8** **SGC**	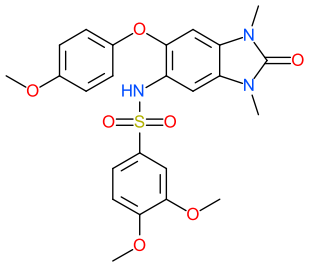	ITC 220nM TRIM24 140nM BRPF1B 1240nM BRPF2	**19**
Family IV ATAD2A	**BAY-850** **Negative control: BAY-460** **SGC**	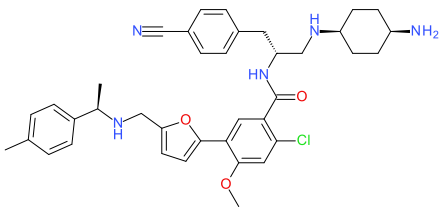	BROMOscan 120nM ATAD2A	**20**
Family VI BAZ2A/B	**BAZ2-ICR** **C, M, T**	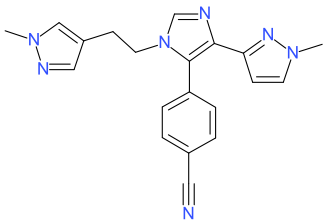	ITC: 109nM BAZ2A 170nM BAZ2B Off-target 1550nM CECR2	**21**
Family VI BAZ2A/B	**GSK2801** **Negative control: GSK8573** **Probe: C, M, T**	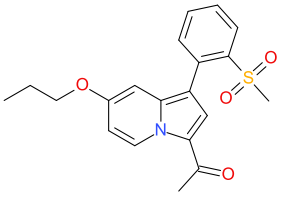	ITC: 257nM BAZ2A 136nM BAZ2B	**22**

Family VIII SMARCA2/4 PB1(5)	**PFI-3** **Negative control: BDF25488524** **Probe: C, M, T** **Control: SGC**	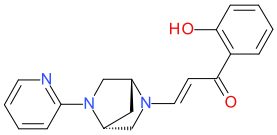	ITC: 89nM SMARCA4 48nM PB1 (5)	**23**

[‡]Cayman Chemical (C), Millipore-Sigma (M), Tocris (T)

References:

1. Moustakim, M. et al. Discovery of a PCAF Bromodomain Chemical Probe. *Angew Chem Int Ed Engl* **56**, 827-831 (2017).
2. Humphreys, P.G. et al. Discovery of a Potent, Cell Penetrant, and Selective p300/CBP-Associated Factor (PCAF)/General Control Nonderepressible 5 (GCN5) Bromodomain Chemical Probe. *J Med Chem* **60**, 695-709 (2017).
3. SGC. NVS-CECR2-1. *https://www.thesgc.org/chemical-probes/NVS-1* (2015).
4. Crawford, T.D. et al. GNE-886: A Potent and Selective Inhibitor of the Cat Eye Syndrome Chromosome Region Candidate 2 Bromodomain (CECR2). *ACS Med Chem Lett* **8**, 737-741 (2017).
5. Filippakopoulos, P. et al. Selective inhibition of BET bromodomains. *Nature* **468**, 1067-73 (2010).
6. Mirguet, O. et al. From ApoA1 upregulation to BET family bromodomain inhibition: discovery of I-BET151. *Bioorg Med Chem Lett* **22**, 2963-7 (2012).
7. Picaud, S. et al. PFI-1, a highly selective protein interaction inhibitor, targeting BET Bromodomains. *Cancer Res* **73**, 3336-46 (2013).
8. Hay, D.A. et al. Discovery and optimization of small-molecule ligands for the CBP/p300 bromodomains. *J Am Chem Soc* **136**, 9308-19 (2014).
9. Picaud, S. et al. Generation of a Selective Small Molecule Inhibitor of the CBP/p300 Bromodomain for Leukemia Therapy. *Cancer Res* **75**, 5106-5119 (2015).
10. Romero, F.A. et al. GNE-781, A Highly Advanced Potent and Selective Bromodomain Inhibitor of Cyclic Adenosine Monophosphate Response Element Binding Protein, Binding Protein (CBP). *J Med Chem* **60**, 9162-9183 (2017).
11. Meier, J.C. et al. Selective Targeting of Bromodomains of the Bromodomain-PHD Fingers Family Impairs Osteoclast Differentiation. *ACS Chem Biol* **12**, 2619-2630 (2017).
12. Bamborough, P. et al. GSK6853, a Chemical Probe for Inhibition of the BRPF1 Bromodomain. *ACS Med Chem Lett* **7**, 552-7 (2016).
13. Bouche, L. et al. Benzoisoquinolinediones as Potent and Selective Inhibitors of BRPF2 and TAF1/TAF1L Bromodomains. *J Med Chem* **60**, 4002-4022 (2017).
14. SGC. TP-472. *https://www.thesgc.org/chemical-probes/TP-472* (2016).
15. Martin, L.J. et al. Structure-Based Design of an in Vivo Active Selective BRD9 Inhibitor. *J Med Chem* **59**, 4462-75 (2016).
16. Clark, P.G. et al. LP99: Discovery and Synthesis of the First Selective BRD7/9 Bromodomain Inhibitor. *Angew Chem Int Ed Engl* **54**, 6217-21 (2015).
17. Theodoulou, N.H. et al. Discovery of I-BRD9, a Selective Cell Active Chemical Probe for Bromodomain Containing Protein 9 Inhibition. *J Med Chem* **59**, 1425-39 (2016).
18. Bamborough, P. et al. A Chemical Probe for the ATAD2 Bromodomain. *Angew Chem Int Ed Engl* **55**, 11382-6 (2016).
19. Bennett, J. et al. Discovery of a Chemical Tool Inhibitor Targeting the Bromodomains of TRIM24 and BRPF. *J Med Chem* **59**, 1642-7 (2016).
20. Fernandez-Montalvan, A.E. et al. Isoform-Selective ATAD2 Chemical Probe with Novel Chemical Structure and Unusual Mode of Action. *ACS Chem Biol* **12**, 2730-2736 (2017).
21. Drouin, L. et al. Structure enabled design of BAZ2-ICR, a chemical probe targeting the bromodomains of BAZ2A and BAZ2B. *J Med Chem* **58**, 2553-9 (2015).

22. Chen, P. et al. Discovery and Characterization of GSK2801, a Selective Chemical Probe for the Bromodomains BAZ2A and BAZ2B. *J Med Chem* **59**, 1410-24 (2016).
23. Fedorov, O. et al. Selective targeting of the BRG/PB1 bromodomains impairs embryonic and trophoblast stem cell maintenance. *Sci Adv* **1**, e1500723 (2015).

Supplementary Table 2

Compound	TTK	CK2A1	CAMK1G	AAK1	ABL1	AURKB	BRAF	CAMKK2	STK10
L-Moses	-0.5	-0.1	-0.3	-1.6	0.0	0.4	-0.1	-0.1	-0.4
I-CBP112	0.0	-1.9	-0.2	-0.7	0.0	0.3	-0.1	-0.4	-0.4
PFI-4	-0.6	-0.5	-0.6	-0.9	0.0	0.4	0.6	0.4	-0.4
LP-99	-0.1	-1.4	-0.2	-0.8	-0.1	0.1	-0.2	0.0	-0.3
PFI-3	-0.7	0.3	0.0	-0.3	-0.1	0.2	-0.1	-0.1	-0.2
NVS-CECR2-1	0.4	-1.0	-0.4	-0.7	0.0	0.3	-0.1	-0.3	-0.1
OF-1	0.1	-2.4	-0.7	-0.9	-0.1	0.3	0.0	-0.3	-0.2
BAY-299	-0.1	-1.4	-0.6	-0.4	0.0	0.2	0.1	-0.4	-0.2
I-BRD9	0.2	-1.1	-0.3	-0.4	0.0	0.2	0.0	-0.2	-0.2
JQ1	-0.5	-1.4	-0.9	-2.8	-0.2	-0.1	-0.4	-0.6	-0.6
GSK6853	0.1	-0.7	-0.5	-0.8	0.1	1.0	0.1	0.5	0.1
TP-472	0.2	-1.1	-0.2	-0.3	0.1	0.2	0.8	0.0	-0.2
BAZ2-ICR	0.3	-1.3	-0.1	0.8	0.0	0.0	0.1	0.0	0.0
SGC-CBP30	-0.4	-1.8	-0.6	-0.6	-0.2	0.0	-0.5	-0.6	0.0
NI-57	0.0	-1.7	-0.6	0.2	-0.1	0.0	0.0	-0.4	0.2
BI-9564	0.1	-1.2	-0.6	0.1	0.0	0.1	-0.2	-0.2	-0.2
GSK2801	0.4	-1.0	-0.3	0.5	0.0	-0.1	-0.3	0.1	-0.5

	EPHA2	FES	GPRK5	GSG2	MERTK	PAK4	MAPK1	MAPK8	STK3
L-Moses	1.1	-0.2	-0.3	0.1	0.0	-0.3	0.1	0.6	0.0
I-CBP112	1.1	-0.1	-0.4	0.1	-0.2	-0.2	0.2	0.3	0.0
PFI-4	1.8	0.0	-0.3	0.3	-0.1	-0.2	0.2	-0.2	0.0
LP-99	0.9	0.0	-0.3	-0.2	-0.2	-0.4	0.2	-0.1	-0.2
PFI-3	-0.2	-0.2	-0.2	0.0	-0.1	-0.2	-0.1	0.1	-0.1
NVS-CECR2-1	1.5	-0.5	-0.1	0.2	0.0	-0.1	0.3	-0.3	-0.1
OF-1	1.2	-0.6	-0.4	0.2	-0.1	-0.2	0.3	-0.1	0.0
BAY-299	2.0	0.0	-0.3	0.1	-0.2	-0.1	0.0	-0.4	0.1
I-BRD9	1.2	0.1	-0.1	0.1	0.0	-0.1	0.1	-0.1	0.1
JQ1	0.9	-0.8	0.1	0.1	-0.3	-0.4	0.2	-0.8	0.1
GSK6853	1.5	-0.2	-0.3	0.6	0.3	0.1	0.2	0.1	0.3
TP-472	2.1	0.0	-0.1	0.1	-0.1	0.0	0.2	0.2	0.1
BAZ2-ICR	1.1	0.0	0.0	0.0	0.0	0.0	0.1	0.2	0.0
SGC-CBP30	1.2	-0.6	0.1	0.0	-0.1	0.0	0.2	0.8	0.0
NI-57	1.5	-0.4	-0.3	0.0	0.0	0.1	0.1	0.1	0.2
BI-9564	2.1	-0.1	-0.4	0.0	0.2	0.0	0.1	0.0	0.0
GSK2801	1.2	-0.2	-0.5	0.2	0.0	-0.2	0.2	0.1	0.1

	CASK	BMX	CSNK1D	DAPK3	DYRK1A	PHGK2	PIM1	RPS6KA1
L-Moses	-0.1	-0.1	0.6	0.2	0.2	-0.1	2.3	0.2
I-CBP112	0.0	-0.1	0.5	0.0	-0.4	0.1	-0.1	0.1
PFI-4	-0.2	0.6	1.3	0.4	-0.5	0.1	0.5	0.1
LP-99	-0.3	0.2	0.2	-0.1	-0.3	-0.1	-0.2	-0.1
PFI-3	-0.2	0.3	0.3	0.0	-0.1	0.1	0.1	-0.2
NVS-CECR2-1	0.1	0.0	0.4	0.7	-0.3	-0.2	0.4	0.2
OF-1	0.0	0.5	0.6	-0.1	-0.8	0.1	-0.2	0.0
BAY-299	-0.1	0.3	1.2	-0.2	-0.5	0.0	-0.2	0.1
I-BRD9	-0.2	0.3	0.0	-0.2	-0.6	0.0	0.1	0.1
JQ1	0.1	-0.3	0.4	-0.1	0.2	-0.3	-0.3	-0.1

GSK6853	0.1	0.3	1.3	1.1	-0.2	0.2	3.7	0.2
TP-472	-0.1	0.5	1.1	0.0	-0.3	0.1	0.4	0.1
BAZ2-ICR	0.2	0.5	0.4	-0.1	-0.1	-0.1	0.2	0.1
SGC-CBP30	0.5	-0.2	0.3	0.2	-0.2	-0.3	-0.2	0.0
NI-57	0.3	0.0	0.6	0.0	0.1	0.1	0.1	0.2
BI-9564	0.0	0.1	1.1	0.1	0.1	-0.1	0.0	0.1
GSK2801	0.5	0.2	0.2	-0.2	0.4	-0.2	-0.3	-0.1

Supplementary table 2: Selectivity screening data (protein kinases): Temperature shift data measured on protein kinases. Shown are average data in Kelvin of three measurements. No significant Tm shifts have been observed.

Supplementary Table 3

Probes	ΔTm (°C) 10µM									
	UHRF1	**RBBP1**	**53BP1**	**BRPF1**	**BRPF3**	**WDR5**	**EED**	**TDRD3**	**FXR1**	**SND1**
BAY-299	NA	-1.0	0.3	-2.5	1.5	0.2	NA	-1.4	0.8	NA
BAY-588	-0.4	-0.1	-2.3	-0.2	NA	-7.3	-0.5	-5.3	-1.2	-1.0
BAY-850	-0.3	-1.0	-0.7	-2.2	-0.4	0.2	NA	-1.8	-1.7	-1.6
BAY-876	-0.2	-0.3	0.0	-0.3	-0.3	0.4	-0.7	-1.0	0.8	-0.9
BI-9564	-0.2	0.0	-0.3	-0.3	-0.6	-0.2	-0.7	-0.6	0.3	-0.9
GSK4027	-0.2	-0.7	-0.1	-0.8	-0.3	0.2	-0.7	-0.6	0.3	-1.0
GSK6853	-0.2	-0.7	-0.1	-0.9	-0.4	0.0	-0.9	-0.7	-1.1	-0.6
GSK8814	-0.2	-0.1	-0.1	-0.2	-0.2	0.2	-0.4	-0.6	0.4	-0.5
I-BRD9	-0.1	0.0	0.1	0.2	0.1	0.1	-0.7	-0.4	0.1	-0.3
I-CBP112	0.0	-0.1	0.3	-0.2	0.0	-0.2	-0.5	-0.6	0.9	-0.7
JQ1	-0.2	-0.7	-0.4	-0.6	-0.7	-0.3	-0.9	-1.4	-0.5	-0.6
L-Moses	NA	-0.4	NA	-2.7	1.0	0.5	-0.3	-0.9	0.3	-1.0
LP99	NA	-0.7	0.3	-2.0	0.0	0.4	-0.2	-0.5	0.1	-0.4
NI57	NA	-0.1	-0.1	NA	-0.4	0.3	-0.4	-0.7	-0.5	-0.4
NVS-CECR2-1	-0.3	-1.0	-0.6	-0.2	-0.3	-0.2	-1.0	-3.3	-5.1	-1.7
OF-1	0.2	-0.7	-0.1	-0.6	0.0	-0.2	-0.7	-1.0	0.7	-0.7
PFI-1	0.2	-0.6	-0.2	-0.3	-0.2	0.0	-0.9	-1.7	-0.1	-0.7
PFI-3	0.5	-0.7	0.1	-0.5	0.4	0.2	-0.9	-0.6	0.4	-0.6
PFI-4	-0.5	-1.2	-0.7	-0.7	0.0	-0.5	-2.2	-1.5	-1.2	-1.1
SGC-CBP30	0.0	-1.2	-0.2	0.6	0.2	0.2	-0.4	-1.1	-1.2	-0.4
TP-238	0.0	-0.4	0.4	-0.3	0.2	0.2	-0.3	-0.7	0.4	-0.5
TP-472	-0.1	-0.5	0.1	0.2	0.3	0.0	-0.5	-0.1	0.8	-0.5

Supplementary Table 3: Selectivity screening data (non-BRD reader domains): Temperature shift assay data of BRD probes screened against a diverse panel of methyl-lysine reader domains. Compounds were screened a concentration of 10 µM. Shown are temperature shifts in Kelvin. No significant Tm shifts have been observed.

Supplementary Table 4

Probes	HATs Activity (%) at 1 and 10 μM									
	EP300		HAT1		MYST1		MYST3		GCN5L2	
	1μM	10μM	1μM	10μM	1μM	10μM	1μM	10μM	1μM	10μM
BAY-299	95	93	100	93	99	99	98	85	99	103
BAY-588	103	99	99	97	100	93	99	96	94	95
BAY-850	98	87	101	101	93	94	96	97	99	102
BAY-876	99	95	97	89	96	91	99	101	100	97
BI-9564	99	94	99	96	106	101	99	100	102	100
GSK4027	93	90	102	89	102	98	101	101	99	102
GSK6853	98	104	100	94	99	101	107	104	107	107
GSK8814	96	102	100	95	99	103	96	102	102	100
I-BRD9	96	99	103	101	104	104	101	99	104	102
I-CBP112	97	99	100	94	98	103	98	99	105	102
JQ1	99	102	98	103	99	95	108	100	104	98
L-Moses	94	90	100	95	97	96	92	90	99	95
LP99	99	98	104	95	90	88	96	100	92	89
NI57	94	93	104	104	96	91	98	99	100	96
NVS-CECR2-1	90	84	99	88	96	94	98	103	100	100
OF-1	100	103	92	93	102	94	100	102	98	93
PFI-1	99	100	102	93	101	95	105	86	96	93
PFI-3	98	97	96	94	99	99	95	96	99	101
PFI-4	99	101	98	96	98	101	97	102	98	96
SGC-CBP30	98	92	96	97	103	97	103	103	101	101
TP-238	99	95	93	100	99	97	97	99	96	92
TP-472	95	96	98	97	100	103	99	98	94	92

Supplementary Table 4: Selectivity screening data (HATs): Effects of BRD probe compounds on the activity of histone acetyltransferases (HATs). Shown are inhibition data (% inhibition) at a compound concentration of 1 μM and 10 μM.

Supplementary Table 5

MTases	MTases Inhibition (%) at 10μM							
	BAY-588	BAY-850	BAY-876	GSK4027	GSK6853	GSK8814	L-Moses	TP-238
ASH1L	-6	3	4	13	4	2	-3	-4
G9A	3	7	-3	1	-2	-2	-3	7
GLP	2	2	0	2	3	2	2	1
MLL1 (Trimeric)	7	-1	11	8	7	6	20	17
MLL3 (pentameric)	7	0	0	2	2	0	1	-3
NSD2	2	-1	0	15	13	24	2	3
NSD1	11	2	2	4	1	19	-6	1
NSD3	-2	14	3	10	7	13	5	15
PRC2-EZH1	3	19	-4	-1	1	1	5	6
PRC2-EZH2	3	3	5	-5	0	2	-4	3
PRDM9	3	10	0	3	-2	0	4	-1
SETD2	0	7	-4	-1	1	7	11	19
SETD7	10	11	10	12	7	7	7	-1
SETD8	-3	2	0	10	-6	-7	-8	-6
SETDB1	5	8	-4	-1	1	1	1	-1
SMYD2	8	19	-10	2	-3	-2	-10	-2
SMYD3	7	6	3	1	9	8	10	7
SUV39H1	12	5	16	-3	-3	-2	-2	-1
SUV39H2	12	-2	-2	5	1	3	5	7
SUV420H1	-5	5	-1	8	5	-3	4	3
SUV420H2	-3	0	-1	-1	-2	0	6	0
DOT1L	3	3	-6	-2	10	5	1	6
PRMT1	0	15	2	4	-7	3	-2	0
PRMT3	5	3	1	2	1	3	0	5
PRMT4	9	25	1	-2	2	1	6	3
PRMT5	4	4	-1	8	3	-2	-3	-12
PRMT6	4	13	-3	6	5	0	5	6
PRMT7	13	3	12	15	11	11	8	9
PRMT8	3	4	9	15	3	5	5	3
PRMT9	3	15	12	8	12	3	13	7
BCDIN3D	16	28	17	14	5	7	9	4
DNMT1	9	4	4	3	-8	-3	3	3
DNMT3A/3L	-1	21	6	3	13	8	2	8
DNMT3B/3L	-6	28	1	1	8	18	-1	0

Supplementary table 5: Selectivity screening data measured against a panel of lysine methyl transferases (MTases). Inhibition (%) was assess at inhibitor concentration of 10 μM. Shown are average values of two measurements.

Supplementary Figure 4

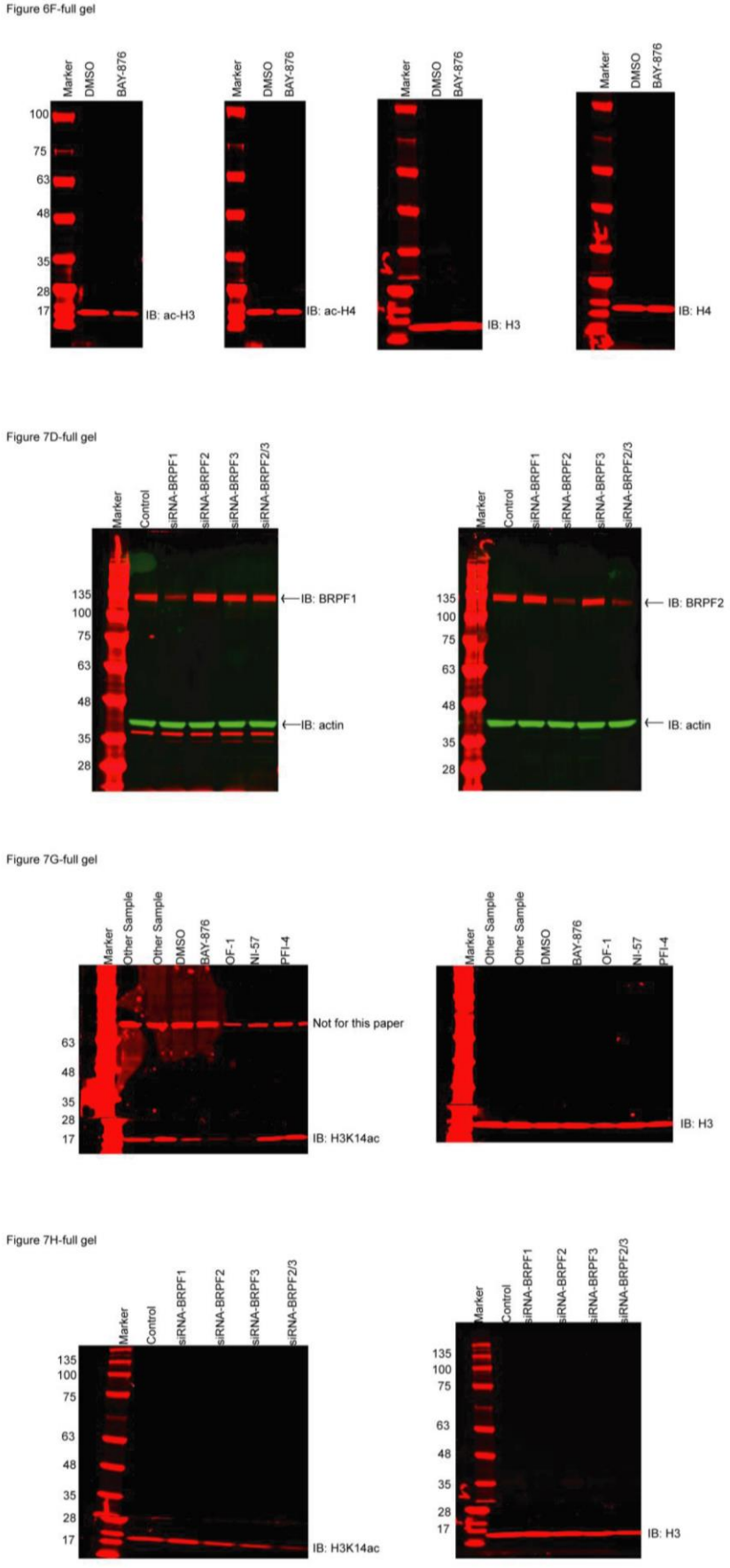

Supplementary Figure 4: Raw data blots used in figure 6 and 7.